

**Fractal-like model of porous silicon**

M. Wesolowski

*Institute of Electronic Materials Technology, ul. Wolczynska 133, 01-919 Warsaw, Poland*

(Received 20 February 2002; revised manuscript received 19 July 2002; published 22 November 2002)

A geometrical model of a porous silicon structure is proposed. The resulting size distribution spectra are analyzed by their relation to photoluminescence and Raman scattering. Both experimental data are investigated and compared to those results. The model well describes the presence of a low-energy part of the photoluminescence spectra with wavelength compatible to bulk crystalline silicon. Shapes and positions of Raman and photoluminescence lines are within the frames of model flexibility and indicate similar values of parameters, especially the minimal size of crystallites where Raman scattering and radiative recombination reveal the activity.

DOI: 10.1103/PhysRevB.66.205207

PACS number(s): 61.46.+w, 61.43.Gt, 63.22.+m, 78.55.Mb

**I. INTRODUCTION**

Since the discovery of visible photoluminescence from porous silicon there have been many investigations concentrated on optical properties of this material. The result is dominating opinion that assumes this effect is due to quantum size-related processes occurring in nanosized remains of silicon, which are formed during anodic etching of wafers.<sup>1</sup> A large number of experimental works reports data that allow to analyze the correlation of nanocrystallite size with photoluminescence. Because this relation revealed by various experiments is not quite clear, many authors try to discuss the nature of this effect and describe it as caused by chemical species of Si-O complexes existing at giant surfaces of material.<sup>2,3</sup> A similar way is to relate the recombination to the presence of radiative defects in the silicon or on the surface.<sup>4-6</sup> Particular behaviors of such defects may lead to insensitivity of the photoluminescence on the crystallite dimension,<sup>7</sup> but it is often neglected that small crystallite size means a high surface/volume ratio and also a resulting short time of consuming it by oxidation, which is apparently a way to decrease size. In such structural conditions that porous silicon represents, it may oppositely occur a decrease of low-dimensional share after the exposition to oxygen. Therefore, from many points of view, a good model of porous geometry, giving the relation between crystallite size and other physical properties of material, could confirm the role of quantum confinement.

An initial model of porous geometry was proposed by Canham in 1990. The existing nanostructural species was established as a system of pores perpendicular to an etched wafer surface.<sup>1</sup> This geometry does not describe the volume morphology of porous silicon well enough to compare microscopy or weight measurements with optical properties. The case in which this material seems to be built within frames of a nanocolumn network is very rare; in general, more complicated structures are observed with a variety of crystallite dimensions. There are some works presuming *a priori* size distribution of crystallites<sup>8,9</sup> but such presumptions usually do not have reliable foundations. On the other hand there are some attempts to analyze more strictly defined geometries,<sup>10</sup> the way of calculating electronic states makes results sensitive to the details of model geometry assump-

tions and makes the discussion and comparison to experimental data difficult. The intent of this paper is to introduce a model of porous geometry corresponding more closely to the real material and to verify it with photoluminescence and Raman experiments in terms of size distribution. This method does not resolve the Schrödinger equation for total structure but it is allowed when crystallites may be approximately treated as insulated.

**II. EXPERIMENTS**

Samples were prepared on a 1- $\Omega$  cm *p*-type silicon wafer in an HF:H<sub>2</sub>O:ethanol=1:1:2 anodic etching solution under a current density of 50 mA/cm<sup>2</sup> for 5 min. After etching, plates were oxidized in a two-step process. The first step used to maintain the porous silicon structure<sup>12</sup> was carried out in a 300 °C oxygen atmosphere for 10 min. The second step was performed to improve surface and structure properties—samples were oxidized in an 800 °C oxygen atmosphere for 20 s. Both steps were executed in the rapid thermal annealing processor. The photoluminescence measurements exhibited a typical for porous silicon, intensive line at 700–900 nm caused, as usually interpreted, by the quantum size effect from smaller crystallites and a second line in the region characteristic for energy gaps of silicon, as presented in Fig. 7 below. Spectra were collected with a cooled germanium detector.

The Raman-scattering experiments were performed with 3.5-eV excitation at room temperature with collection by a charge coupled device camera. An asymmetric line at about 500 cm<sup>-1</sup> was observed, as shown in Fig. 6 below. The initial half width of 8.2 cm<sup>-1</sup> was noticed for the bulk crystalline substrate.

The spectra were typical for such substrates and etching conditions. The second photoluminescence line is usually not observed with spectra measured by photomultipliers that are usually blind to wavelengths higher than 0.9–1  $\mu$ m.

**III. MODEL DESCRIPTION**

Typical porous silicon formation as indicated by electron microscopy<sup>13</sup> is constructed in a more complex manner than the simple type of representative nanocrystals surrounding

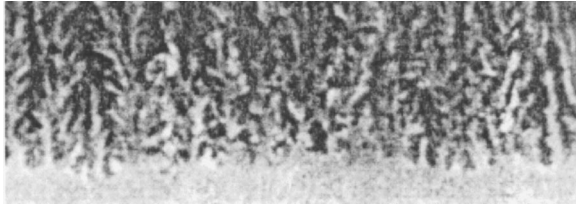


FIG. 1. Cross-sectional scanning electron microscopy photograph of a porous silicon layer, from Ref. 13.

columnar pores. It seems that the most dominant structure occurs when the primary pore, which is perpendicular to the surface, has microns of length and generates a second generation of smaller pores, which generates the next one, etc. Smaller pores are about perpendicular to pores of the previous file—the exemplary morphology is presented in Fig. 1. Sometimes a few generations of pores are visible. Often microscopy photographs give a view of a spongelike structure.

Let consider the pore system model as shown in Fig. 2. The largest first-order pore produces perpendicular pores with proportionally smaller sizes, each of them generating the next perpendicular pores, etc. This system suggests a fractal-like structure that seems to be close to observed pore networks and, as demonstrated, can give a solution of the size distribution problem, explained by experimental photoluminescence and Raman results.

Let us state that each pore has the shape of parallelepiped with a square base and a proportion of the shorter to the longer edge equal to  $c$ . It generates  $n$  pores  $k$ -times smaller in dimension. Let the initial pore width (shorter edge of first-order pore) be  $x_0$ , the next  $x_1 = x_0/k$ , and so on. Then the dimension of pores  $x_m$  will be  $x_m = x_0(1/k)^m$ , their number is  $n_m = n^m$ , and their entire volume

$$v_m = n^m \frac{x_0}{c} \left(\frac{1}{k}\right)^m \left[ x_0 \left(\frac{1}{k}\right)^m \right]^2 \approx \left(\frac{n}{k^3}\right)^m. \quad (1)$$

The factor  $n/k^3$  could be treated as a material coefficient depending on the real morphological structure.

For further calculations the problem can be made continuous and the total volume of etched-from-one-pore material can be calculated as a function of the pore dimension  $x$  and other model parameters:

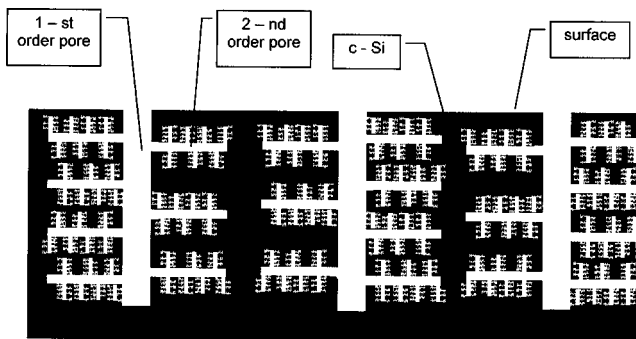


FIG. 2. Proposed porous silicon structure network: cross section of the layer.

$$\begin{aligned} v &= \sum_{m=0}^{\infty} v_m \cong \int_0^{\infty} v(m) dm = \int_{x_0}^0 v(x) \left( -\frac{1}{x \ln k} \right) dx \\ &= \int_0^{x_0} v'(x) dx, \end{aligned} \quad (2)$$

where  $v'(x)$  is the volume density for considered pores of size  $x$ , meaning the volume of pores of  $x$  in dimensions per unit of size dimension

$$v'(x) = \frac{1}{c} x_0^{\ln n / \ln k} \left( \frac{1}{\ln k} \right) x^{2 - (\ln n / \ln k)}. \quad (3)$$

The volume  $v$  in both discrete and integral calculations becomes finite under the condition

$$\frac{n}{k^3} < 1,$$

so

$$\frac{\ln n}{\ln k} < 3.$$

The behavior of factor  $v'(x) \approx x^{2 - (\ln n / \ln k)}$  exhibits powerlike dependency with the index varying from  $-1$  to  $2$ . Commonly used material coefficients to describe the porous structure is the porosity, defined as the ratio of empty volume to the total volume of a material (porosity presumed this way is  $0 < p < 1$ ). It's convenient to normalize the integral (2) to  $p$  through multiplication of  $v'$  by the number  $N$  of first-order pores in a unit volume and divide it by unit volume to obtain the desired value of porosity instead of the total volume etched from one pore:

$$V'(x) = N \cdot v'(x) / \text{cm}^3$$

with

$$\int_0^{x_0} V'(x) dx = p.$$

The final formula for  $V'(x)$  can be written as

$$V'(x) = p \cdot (3 - \ln n / \ln k) \cdot x_0^{(\ln n / \ln k) - 3} \cdot x^{2 - \ln n / \ln k} \quad (4)$$

and it means the volume of pores of size  $x$  per unit size per unit volume.

Electron microscopy indicates that filled and empty volumes are similar in shape and measure, meaning that the overall view is similar to the one presented in Fig. 1, in which exchanging etched volume and the remaining material do not affect the view. The real conditions suggest the assumption that the distribution of etched volume is similar to the distribution of the remaining size, so assigning  $V'$  to the remaining silicon volume can be done. Therefore, below,  $V'$  will designate the “volume density” of remaining silicon. Obviously  $p$  should be replaced by  $1 - p$ :

$$V'(x) = (1 - p) \cdot (3 - \ln n / \ln k) \cdot x_0^{(\ln n / \ln k) - 3} \cdot x^{2 - (\ln n / \ln k)}. \quad (5)$$

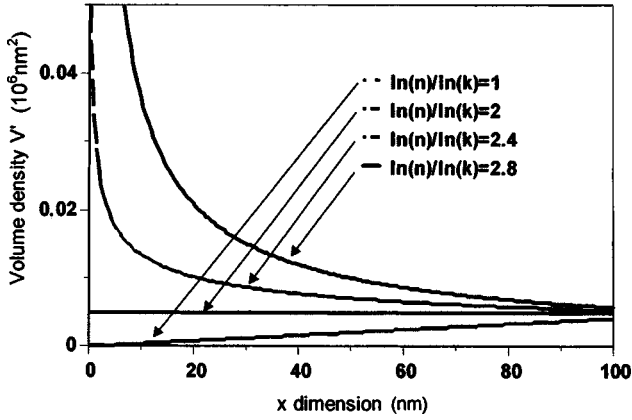


FIG. 3. Resulting distribution profiles for various  $\ln(n)/\ln(k)$  ratios,  $x_0 = 100$  nm. To make the picture more clear, particular curves (except the curve for  $\ln n/\ln k=2$ ) are arbitrary normalized to the same value at  $x=120$  nm.

The “volume density” of silicon remains  $V'$  versus crystallite size  $x$  for  $x_0 = 100$  nm, and a few values of  $\ln n/\ln k$  is shown in Fig. 3. The structure allows to find quite different distributions with an increase in the volume of the pores with a decrease of the size, or the opposite.

#### IV. PHOTOLUMINESCENCE AND RAMAN SPECTRA

It is possible to calculate electronic states of such a structure directly by resolving the Schrödinger equation as in Ref. 11, but this is not the aim of this paper. When the proportion of length to cross-sectional dimension is high, crystallites may be treated as insulated and simple evaluation of the photoluminescence may proceed.

The only structural parameter used in this evaluation is the size distribution. The photoluminescence intensity spectra  $I(E)$  should be in such circumstances in accordance with the formula

$$I(E_g) \approx \frac{1}{\tau(E_g)} V'(x) \left| \frac{dx(E_g)}{dE_g} \right| \cdot S, \quad (6)$$

where  $1/\tau(E_g)$  is the radiative recombination rate corresponding to a given crystallite energy gap and  $x(E_g)$  is the dependence of the crystallite dimension on its energy gap. The factor  $S$  arises from the nonradiative recombination that could be size dependent especially in case of surface-related recombination. This recombination may be evaluated as proportional to the surface/volume ratio, so it is proportional to the reverse of  $x$ .

This paper will not concentrate on the  $\tau(E_g)$  and  $x(E_g)$  calculations that are provided in usually tight-binding<sup>7,15</sup> local-density approximation<sup>16,17</sup> and linear combination of atomic orbitals<sup>14</sup> or effective-mass approximations.<sup>8</sup> The  $\tau$  value used was determined according to the tight binding calculations. However, the evaluation depends on the crystallite geometry; results based on quantum dot and quantum wire geometry turn out not to be very significantly different. Our case is an intermediate one, so in a first approximation a

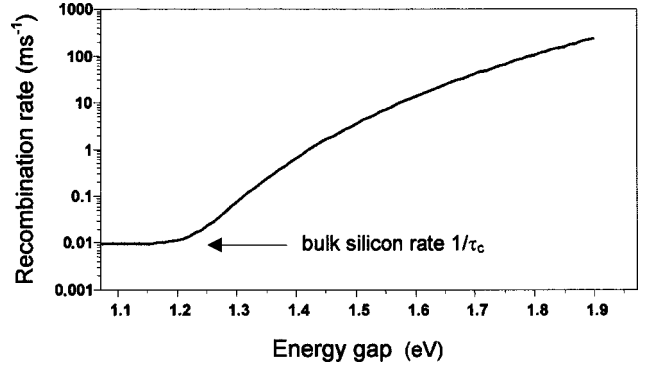


FIG. 4. Applied recombination rate vs energy-gap dependence for silicon spheres; in related calculations the bulk silicon radiative lifetime  $\tau_c$  was a variable parameter.

spherical shape can be used. The dependence of the radiative recombination rate on the particles’ energy gap applied for further evaluation is shown in Fig. 4.

The  $x(E_g)$  relation may be simply derived according to the effective-mass approximation.<sup>8</sup> Here the change from spherical to a wire geometry leads to a relatively small ( $\frac{1}{3}$ ) decrease of the confinement energy, and as mentioned, the spherical shape was chosen. The result of  $I(E_g)$  calculations based on these relations for a few values of the parameter  $\ln(n)/\ln(k)$  and  $x_0 = 100$  nm is shown in Fig. 5.

Because of the limitation of applied approximations at low dimensions, to obtain photoluminescence spectra describing the porous silicon structure, the minimum value of the  $x$  dimension should be used. The spectra should be a suitable cutoff at a corresponding wavelength.

The same procedure may be carried out for Raman scattering. The intensity formula should be taken into account:

$$I(\omega) \approx \int V'(x) I(\omega, x) dx, \quad (7)$$

where  $I(\omega)$  is the Raman-scattering cross section relative to the given wavelength, and  $I(\omega, x)$  is the cross section corresponding to a wavelength and a crystallite size.

$I(\omega, x)$  may be resolved in terms of spherical Gaussian phonon confinement,<sup>18</sup> which analyzes the contribution of

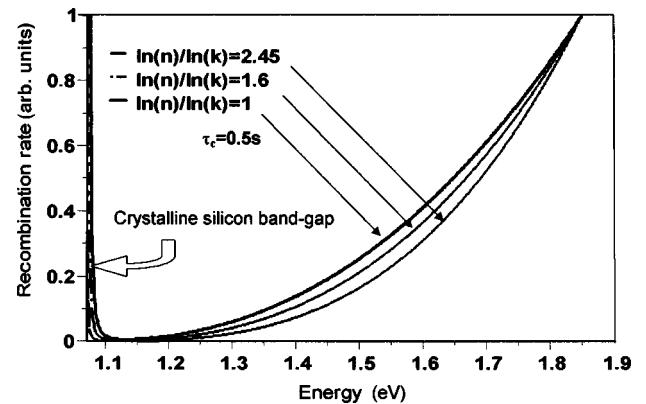


FIG. 5. Calculated recombination curves  $I(E_g)$  for the porous structure. The bulk radiative time  $\tau_c = 0.5$  s was used. Curves are normalized to the same value at 1.85 eV.

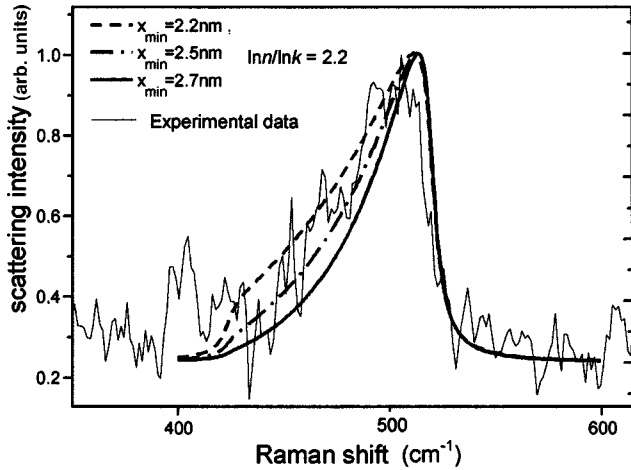


FIG. 6. Experimental spectra of Raman scattering of porous silicon together with calculated spectra for three cutoff sizes.

non- $k=0$  phonons in the scattering process. The phonon wave function in crystallite of diameter  $L$  may be described in the form

$$\Psi(q_0, r) = W(r, L) \cdot \Phi(q_0, r), \quad (8)$$

where  $W(r, L)$  is the envelope function and  $\Phi(q_0, r)$  the wave function of the  $q_0, r$  phonon in an infinite crystal. The  $W(r, L)$  function for the spherical crystallite may be set as the Gaussian

$$W(r, l) = \exp(-8r^2/L^2). \quad (9)$$

Calculated spectra for the proposed model of the size distribution  $V'(x)$  are shown in Fig. 6. The initial half width of  $8.2 \text{ cm}^{-1}$  of a crystalline phonon line was taken according to its value from bulk experimental data.

Similarly as for the photoluminescence, Raman spectra are sensitive to the smallest dimension limit. It is characteristic for Raman spectra, in comparison to the photoluminescence, that parts originating from nanocrystallites and larger crystallites are not clearly distinguishable. The low size limit in this model is similar to the value from the case of effective-mass approximation for electron confinement—crystallites discontinue to be described by crystal approximations for sizes smaller than 1.5 nm.

Both photoluminescence and Raman spectra estimations can be compared to experimental data. The photoluminescence fit shown in Fig. 7 is built by a modulation of curves from Fig. 5 by Gauss lines of half width of 70 meV. The fit requires a value of the ratio of bulk silicon lifetime to the lifetime of a 2.3-nm crystallite on the level of  $3 \times 10^5$  and the cutoff size 2.3 nm. The  $\ln n / \ln k$  ratio best value is 1.6.

The Raman-scattering fits (Fig. 6) are strongly sensitive on the smallest dimension cutoff; the resulting best fit gives almost as high as possible a ratio of  $\ln n / \ln k$  and a smallest dimension equal to 2.5 nm. Both results are in agreement with photoluminescence; the minimal  $x$  dimensions are almost identical.

The lower bulk to nanocrystalline lifetime ratio in the photoluminescence fitting is possible to obtain for higher

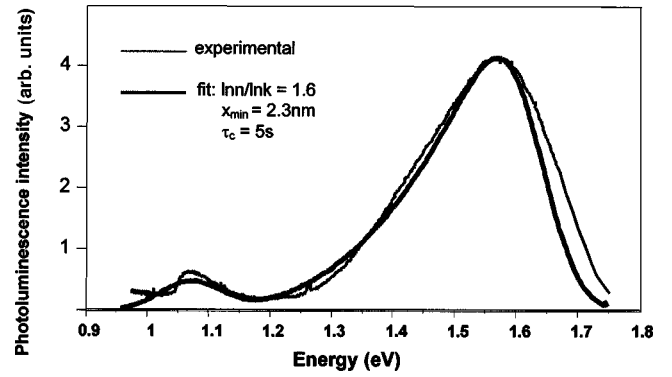


FIG. 7. Experimental spectra and calculated fit of porous silicon photoluminescence.

$\ln n / \ln k$  values. When  $\ln n / \ln k = 2.2$ , lifetime ratios reach  $8 \times 10^4$  and the curve only slightly worse corresponds in the middle region to experiments.

It may be interesting to compare those results to work presented in Ref. 11, describing the photoluminescence calculation for Gaussian size distribution related to plasma-enhanced chemical-vapor deposition silicon nanocrystals embedded in  $\text{SiO}_2$ , where a satisfying fit was obtained for oscillator strength vs energy shift dependence as

$$1/\tau \approx \Delta E^{4.5}. \quad (10)$$

The applied formula (Fig. 4) is the type  $1/\tau \approx \Delta E^{5.6}$  in the important region. A weaker dependence will make easier to fit at higher  $\ln n / \ln k$  values. That will be in coherence with the Raman fit that may seem as more independent of presumptions.

As proposed by other authors, size distributions of porous silicon are dominated by logarithmic, logarithmic-normal,<sup>9</sup> or sometimes Gaussian<sup>8,19</sup> distributions. The presence of a low-energy emission line in photoluminescence suggests a fraction of large dimension crystallites and makes a typical Gaussian distribution disputable. The logarithmic-normal distribution

$$V'(x) \approx \exp\left\{-\frac{1}{2\sigma^2} \left[\ln\left(\frac{x-x_0}{\mu}\right)\right]^2\right\} \quad (11)$$

may be similar to some presented above when the initial dimension  $x_0$  is very small. Simple logarithmic distributions can be close to those proposed. The Raman spectra requires a high fraction of low-dimensional crystallites, suggesting a large value of  $\ln n / \ln k$ . This type of distribution (Fig. 3) with a sufficient fraction of large sizes to obtain adequate photoluminescence is somewhat difficult to build on the basis of logarithmic, logarithmic-normal, or Gaussian functions.

## V. CONCLUSIONS

A fractal-like model of a porous silicon structure was proposed and compared to optical measurements. Experiments indicated nanocrystallite and larger crystallite activity in agreement with calculations. Performed fits of model parameters to measured Raman and photoluminescence spectra

lead to similar values, establishing almost the same minimal crystallite size. Because of the sensitivity of the photoluminescence spectra on the radiative lifetime of nanocrystals the successful fit indicates the validity of applied lifetimes. In

summary, obtained results disclosed support the idea of the existence of optically active nanocrystals exhibiting quantum size effects and demonstrated a geometrical interpretation of the size distribution problem.

- 
- <sup>1</sup>L. T. Canham, *Appl. Phys. Lett.* **57**, 1046 (1990).
  - <sup>2</sup>M. S. Brandt, H. D. Fuchs, M. Stutzman, J. Weber, and M. Cardona, *Solid State Commun.* **81**, 307 (1992).
  - <sup>3</sup>D. W. Cooke, B. L. Bennett, E. H. Farnum, W. L. Hulst, K. E. Sickafus, J. F. Smith, T. N. Taylor, P. Tiwiari, and A. M. Portis, *Appl. Phys. Lett.* **68**, 1663 (1996).
  - <sup>4</sup>H. J. von Bardeleben, D. Stievenard, A. Grossman, C. Ortega, and J. Siejka, *Phys. Rev. B* **47**, 10 899 (1993).
  - <sup>5</sup>S. M. Prokes and O. J. Glembocki, *Phys. Rev. B* **49**, 2238 (1994).
  - <sup>6</sup>G. G. Quin and Y. Q. Jia, *Solid State Commun.* **86**, 559 (1993).
  - <sup>7</sup>M. V. Wolkin, J. Jorne, P. M. Facht, G. Allan, and C. Delerue, *Phys. Rev. Lett.* **82**, 197 (1999).
  - <sup>8</sup>G. Fishman, I. Mihalcescu, and R. Romestain, *Phys. Rev. B* **48**, 1464 (1993).
  - <sup>9</sup>H. Yorikawa and S. Muramatsu, *Appl. Phys. Lett.* **71**, 644 (1997).
  - <sup>10</sup>B. Sapoval, S. Russ, and J-N Chazalviel, *J. Phys.: Condens. Matter* **8**, 6235 (1996).
  - <sup>11</sup>P. F. Trwoga, A. J. Kenyon, and C. W. Pitt, *J. Appl. Phys.* **83**, 3789 (1998).
  - <sup>12</sup>J. L. Bastson, M. A. Tischler, and R. T. Collins, *Appl. Phys. Lett.* **62**, 2667 (1993).
  - <sup>13</sup>J. P. Gonchond, A. Halimanoui, and K. Ogura, *Microscopy of Semiconducting Materials* (Institute of Physics, University of Reading, Berkshire, 1991), p. 235.
  - <sup>14</sup>G. D. Sanders and Yia-Chung Chang, *Phys. Rev. B* **45**, 9202 (1992).
  - <sup>15</sup>M. Lanoo and J. Bourgoin, *Point Defects in Semiconductors I*, edited by M. Cardona (Springer-Verlag, New York, 1981).
  - <sup>16</sup>C. G. Van de Walle and J. E. Northrup, *Phys. Rev. Lett.* **70**, 1116 (1993).
  - <sup>17</sup>K. Takeda and K. Shiraishi, *Phys. Rev. B* **39**, 11 028 (1989).
  - <sup>18</sup>I. H. Campbell and P. M. Fauchet, *Solid State Commun.* **58**, 739 (1986).
  - <sup>19</sup>E. P. O'Reilly and A. R. Adams, *IEEE J. Quantum Electron.* **30**, 366 (1994).